Ultrasonic attenuation due to phonon–phonon interaction, thermoelastic loss and dislocation damping in transition metal carbides

2008 J. Phys.: Condens. Matter 20 345227

(http://iopscience.iop.org/0953-8984/20/34/345227)

IOP PUBLISHING JOURNAL OF PHYSICS: CONDENSED MATTER

J. Phys.: Condens. Matter **20** (2008) 345227 (6pp) doi:10.1088/0953-8984/20/34/345227

Ultrasonic attenuation due to phonon–phonon interaction, thermoelastic loss and dislocation damping in transition metal carbides

R K Singh, R P Singh, M P Singh and P C Srivastava

Department of Physics, Banaras Hindu University, Varanasi-221005, India

E-mail: rksingh_17@rediffmail.com

Received 2 February 2008, in final form 15 July 2008
Published 6 August 2008
Online at stacks.iop.org/JPhysCM/20/345227

Abstract

Temperature dependent ultrasonic attenuation due to phonon–phonon (p–p) interaction, thermoelastic loss and dislocation damping due to screw and edge dislocations have been investigated in fcc (NaCl B1 type) structured group IVb and Vb monocarbides (transition metal carbides, namely TiC, ZrC, HfC, VC, NbC and TaC) in the temperature range 50–500 K, along the three crystallographic directions of propagation, namely [100], [110] and [111] for longitudinal and shear modes of propagation. The second- and third-order elastic moduli (SOEM and TOEM) obtained at different temperatures using the electrostatic and Born repulsive potentials and taking interactions up to next-nearest neighbours, have been used to obtain Gruneisen numbers, acoustic coupling constants and their ratios along different directions of propagation and polarization for longitudinal and shear modes of wave propagation. Temperature variation of the phonon relaxation time shows exponential decay. The results have been discussed and compared with available data.

1. Introduction

Transition metal carbides (TMCs) are metallic compounds with outstanding properties, e.g. they are extremely hard and have very high melting temperatures. For instance, the melting temperature of TaC (about 4200 °C) is the highest amongst known materials. TMCs are chemically very stable and have high corrosion resistance. Due to these properties they are widely used in industry as cutting tools. They have also potential applications in information storage technology (for coating magnetic sheets), high power energy industry and optoelectronics. Carbides of transition metals, with MX (M = Ti, Zr, Hf, V, Nb and Ta, X = C) stoichiometry are usually cubic, where the metallic atoms form the face-centred cubic (fcc) sub-lattice, and nonmetallic atoms occupy interstitial positions, forming the NaCl (B1) type structure [1]. Recently, TMCs have attracted increasing attention among researchers due to their excellent thermal stability and chemical inertness to copper at elevated temperatures [2].

In the recent past, extensive work on phonon-related properties, electronic structure, lattice dynamics and structural and elastic properties of these transition metal carbides have been done [1–8], but ultrasonic attenuation studies, which provide very important information regarding microstructure and other properties, have not been carried out on these TMCs. So, we have chosen this important class of compounds to study the temperature variation of ultrasonic attenuation and related parameters. In the present paper, using simple potentials namely electrostatic and Born repulsive potentials, SOEM and TOEM have been obtained at different temperatures, which in turn have been used to evaluate ultrasonic attenuation and related parameters, namely Gruneisen parameters and nonlinearity coupling constants, over a wide temperature range of 50–500 K. Temperature dependence of the attenuation behaviour has been given for longitudinal and shear waves along different directions of propagation.

The study of temperature-dependent ultrasonic attenuation plays a very important role in understanding the interaction of ultrasonic waves with crystals. Changes in ultrasonic attenuation with temperature can be used to infer information about the interaction of ultrasonic waves with individual phonons in the region $\omega\tau \ll 1$ [9], where ω is the angular

frequency and τ is the thermal relaxation time. Different causes can be attributed to the attenuation of ultrasonic waves propagating through them: of these, important causes of acoustical dissipation are phonon–phonon (p–p) interaction, thermoelastic loss, dislocation damping due to screw and edge dislocations, scattering from grain boundaries (dominant in polycrystalline materials), etc. The phonon–phonon interaction is the dominant cause of ultrasonic attenuation at room temperature and above in all types of solids, i.e. metallic, semiconducting and dielectrics [10–13]. Attenuation due to thermoelastic loss is negligible compared to total attenuation. The phonon–phonon interaction gives rise to the energy loss of ultrasonic waves whose estimation is possible using Meson's approach [14–20].

2. Computational detail

2.1. Elastic constants

Second- and third-order elastic moduli (SOEM and TOEM), C_{ij}^0 and C_{ijk}^0 at 0 K, have been obtained using electrostatic and Born–Mayer potentials and following Brugger's definition of elastic constants [21]. Repulsive parameters and nearest-neighbour distances have been used as input data and interactions up to next-nearest neighbours have been considered. According to Brugger's definition, the nth-order elastic constant is defined as

$$C_{ijklmn\cdots} = \left(\partial^n u/\partial\varepsilon_{ij}\partial\varepsilon_{kl}\partial\varepsilon_{mn}\ldots\right) \tag{1}$$

where u is the crystal free-energy density and ε_{ij} is the strain tensor in Voigt notation.

For cubic crystals, three independent SOEM (C_{11}, C_{12} and C_{44}) and six independent TOEM (C_{111}, C_{112}, C_{144}, C_{166}, C_{456} and C_{123}) occur. Temperature variation of SOEM and TOEM has been obtained by adding a vibrational contribution to elastic constants. According to lattice dynamics developed by Leibried *et al* [22] and Ludwig *et al* [23], temperature variation of SOEM and TOEM has been obtained by adding a vibrational contribution to elastic constants, using the theories tested by us for evaluating acoustical dissipation for other fcc and bcc structured compounds [10–13]. SOEM and TOEM at any temperature are obtained by adding corresponding vibrational contributions to SOEM and TOEM at absolute zero, namely C_{ij}^0 and C_{ijk}^0, i.e.

$$C_{ij}(T) = C_{ij}^0 + C_{ij}^{\text{vib}} \tag{2}$$

$$C_{ijk}(T) = C_{ijk}^0 + C_{ijk}^{\text{vib}} \tag{3}$$

where C_{ij}^{vib} and C_{ijk}^{vib} are vibrational contributions to the elastic constants.

2.2. Ultrasonic attenuation

In the Akhiezer regime ($\omega\tau \ll 1$), a sound wave passing through a solid can be attenuated by two processes [16]. First, if the wave is longitudinal, periodic contractions and dilations in the solid induce a temperature wave via thermal expansion. Energy is dissipated by heat conduction between regions of different temperatures. This is called thermoelastic loss. Second, dissipation occurs as the gas of thermal phonons tries to reach an equilibrium characterized by a local (sound-wave-induced) strain. This is the internal friction mechanism.

The physical basis for obtaining the attenuation coefficient is that the elastic constants contributed by the thermal phonons relax [14–20]. The phonon contribution to the unrelaxed elastic constants is obtained by taking into consideration the change in energy of the thermal phonons due to applied instantaneous strain. The frequency of each mode ν_i is changed by $\frac{\partial\nu_i}{\nu_i} = -\gamma_i^j S_j$, where γ_i^j is the generalized Gruneisen parameter and S_j is the instantaneous strain. It is assumed that all the phonons of a given direction of propagation and polarization have equal change in frequency. Then phonons of the ith branch and the jth mode suffer a change in temperature $\frac{\Delta T_i}{T_0} = -\gamma_i^j S_j$ (T is the temperature). A relaxed elastic constant is obtained after there is phonon–phonon coupling among various branches and the ΔT_i relax to a common temperature change, ΔT, given by $\frac{\Delta T}{T} = -\langle\gamma_i^j\rangle S_j$, where $\langle\gamma_i^j\rangle$ is the average value of γ_i^j. The thermal relaxation time is

$$\tau = \tau_s = \frac{\tau_{\text{l}}}{2} = \frac{3K}{C_v\langle V\rangle^2} \tag{4}$$

where K is thermal conductivity, C_v is specific heat per unit volume and $\langle V\rangle$ is Debye average velocity.

According to Mason and Bateman [16], SOEM and TOEM are related by the Gruneisen parameter γ_i^j and hence by the nonlinearity parameter, Γ (which is a measure of anharmonicity of the crystal). Ultrasonic attenuation due to phonon–phonon interaction in the Akhiezer regime ($\omega\tau \ll 1$) is given by

$$\alpha_{\text{p-p}} = \frac{2\pi^2 f^2 \Gamma E_0 \tau}{3\rho V^3} \tag{5}$$

where the nonlinearity coupling constant is

$$\Gamma = 9\langle(\gamma_i^j)^2\rangle - \frac{3\langle\gamma_i^j\rangle^2 C_v T}{E_0} \tag{6}$$

$\langle(\gamma_i^j)^2\rangle$ and $\langle\gamma_i^j\rangle$ are square average and average square Gruneisen parameters, V is sound wave velocity for longitudinal waves (V_{l}) and for shear waves (V_{s}) and ρ is density.

The Debye average velocity is given by

$$\frac{3}{(\langle V\rangle)^3} = \frac{1}{V_{\text{L}}^3} + \frac{2}{V_{\text{S}}^3}. \tag{7}$$

Propagation of a sound wave through a crystal produces compression and rarefactions. As a result heat is transmitted from the compressed region (at higher temperature) to the rarefied region (at lower temperature) and hence thermoelastic loss occurs, which is given by

$$\alpha_{\text{th}} = \frac{4\pi^2 f^2 \langle\gamma_i^j\rangle^2 KT}{2\rho V_{\text{L}}^5}. \tag{8}$$

Dislocation damping due to screw and edge dislocations also produces appreciable loss due to phonon–phonon interactions.

Table 1. Calculated and experimental [1, 2] second-order elastic constants in (10^{12} dyn cm^{-2}) and hardness parameter, q(Å), of transition metal carbides at 300 K.

	C_{11}		C_{12}		C_{44}		
	Present	Expt.	Present	Expt.	Present	Expt.	q (Å)
TiC	5.13	5.13	1.67	1.06	1.71	1.78	0.3487
ZrC	4.70	4.70	1.08	1.00	1.20	1.60	0.3399
HfC	5.00	5.00	1.23	1.05	1.25	1.80	0.3321
VC	5.00	5.00	3.52	2.90	3.54	1.50	0.4239
NbC	6.20	6.20	2.46	2.00	2.48	1.50	0.3823
TaC	5.50	5.50	2.49	1.50	2.50	1.90	0.4002

Table 2. Calculated phonon viscosity due to screw and edge dislocation of transition metal carbides at 300 K for longitudinal (in cp) and shear (in mp) waves.

	δ_{screw}		δ_{edge}	
	Long.	Shear	Long.	Shear
TiC	0.191	0.142	0.358	0.517
ZrC	0.322	0.143	0.726	0.916
HfC	0.810	0.327	0.186	0.229
VC	0.231	0.464	0.275	0.648
NbC	0.213	0.214	0.350	0.563
TaC	0.339	0.396	0.513	0.881

The loss due to this mechanism can be obtained by multiplying dislocation viscosities by the square of the dislocation velocity.

Dislocation damping due to screw and edge dislocations is given by [13]

$$\delta_{screw} = 0.071\zeta \tag{9a}$$

$$\delta_{edge} = 0.053\zeta/(1-\sigma^2) + 0.0079/(1-\sigma^2)(\Phi/\Lambda)\psi \tag{9b}$$

where

$$\psi = \zeta_l - (4/3)\zeta_s, \qquad \zeta_l = E_0\Gamma_l\tau/3, \qquad \zeta_s = E_0\Gamma_s\tau/3$$

$$\Lambda = (C_{11}+2C_{12})/3, \qquad \Phi = (C_{11}-C_{12}+C_{44})/3$$

and

$$\sigma = C_{12}/(C_{11}+C_{12})$$

where Λ, Φ, ζ, σ and ψ are the bulk modulus, shear modulus, phonon viscosity, Poisson's ratio and compressional viscosity, respectively. C_{ij}s are the second-order elastic constants.

3. Results and discussion

SOEM and TOEM have been obtained at different temperatures using equations (2) and (3). Lattice parameters and hardness parameters [1, 2] have been used as input data. Values of SOEM obtained using the present approach have been compared with available theoretical and experimental values (see table 1) and are in good agreement with experimental values, except for minor disagreement in C_{12} and C_{44} values, which may be attributed to the difference in the input parameters used. Incorporating interactions beyond next-nearest neighbour may lead to better agreement between calculated and experimental values of shear moduli. Our calculations of second- and third-order elastic moduli are reasonable since we have made an '*ab initio*' determination of elastic moduli of these transition metal carbides at different temperatures. There are no elastic data as a function of temperature for these compounds. Most simple theories are able to get a reasonable estimate of elastic moduli at room temperature only by using experimental parameters. Thus the present approach for evaluation of SOEM and TOEM is valid.

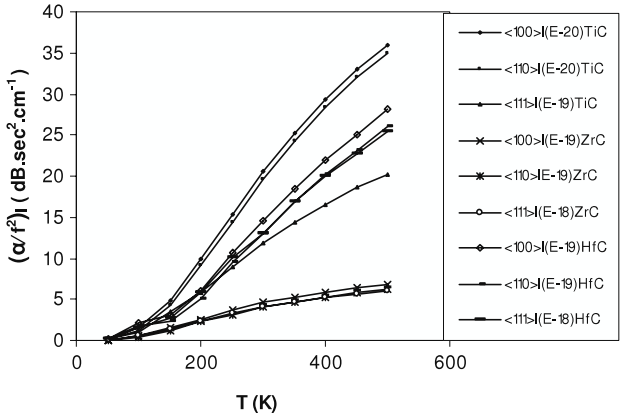

Figure 1. Temperature variation of $(\alpha/f^2)_l$ along different directions of propagation of the group IV carbides. Curves along ⟨110⟩ (—∗—) and ⟨111⟩ (—o—) for ZrC and along ⟨110⟩ (— - —) and ⟨111⟩ (——) for HfC overlap (however, for values of (α/f^2) along ⟨110⟩ the multiple is (E-19) while along ⟨111⟩ the multiple is (E-18) for both compounds i.e. values of (α/f^2) are different).

SOEM and TOEM values have been used to obtain the squared average Gruneisen number, $\langle\gamma_i^{j2}\rangle$, average squared Gruneisen parameter, $\langle\gamma_i^j\rangle^2$ for longitudinal and shear waves, nonlinearity coupling constants Γ_l, Γ_s and Γ_s^* (which are measures of the anharmonicity of the lattice) and their ratios Γ_l/Γ_s and Γ_l/Γ_l^* along different directions of propagation as given in table 3. Values of the ratio of the nonlinearity constants along ⟨100⟩ and ⟨110⟩ are as expected [18]. Dislocation damping due to screw and edge dislocations, (δ_{screw} and δ_{edge}) have been evaluated using equations (9*a*) and (9*b*), as presented in table 2.

Ultrasonic attenuation due to phonon–phonon interaction for longitudinal and shear waves, $[(\alpha/f^2)_l$ and $(\alpha/f^2)_s]$ have been evaluated using equation (5). Temperature variation of $(\alpha/f^2)_l$ and $(\alpha/f^2)_s$ along the [100], [110] and [111] directions of propagation are shown in figures 1–4.

Table 3. Calculated squares average Gruneisen number for longitudinal wave $\langle\gamma_i^{j2}\rangle_l$, average squared Gruneisen parameter for longitudinal wave $\langle\gamma_i^{j}\rangle_l^2$, and for shear wave $\langle\gamma_i^{j}\rangle_{s,}^2\langle\gamma_i^{j}\rangle_{s*}^2$, nonlinearity coupling constants Γ_l, Γ_s and nonlinearity coupling constants ratios Γ_l/Γ_s, Γ_l/Γ_{s*} of transition metal carbides at 300 K. (Note: s—polarization along [001]; s*—polarization along [1$\bar{1}$0].)

		$\langle\gamma_i^{j2}\rangle_l$	$\langle\gamma_i^{j}\rangle_l^2$	$\langle\gamma_i^{j}\rangle_s^2$	$\langle\gamma_i^{j}\rangle_{s*}^2$	Γ_l	Γ_s	Γ_{s*}	Γ_l/Γ_s	Γ_l/Γ_{s*}
TiC	[100]	4.31	1.59	0.23	—	28.07	2.09	—	13.37	—
	[110]	4.53	2.08	1.35	7.83	26.74	12.23	70.79	2.18	0.37
	[111]	22.96	6.81	3.98	4.41	160.67	35.89	39.72	4.47	4.04
ZrC	[100]	4.76	1.50	0.16	—	33.77	1.50	—	22.45	—
	[110]	4.62	1.99	1.04	9.17	30.02	9.44	82.61	3.17	0.36
	[111]	39.65	9.39	4.66	6.64	302.05	42.02	59.84	7.18	5.04
HfC	[100]	4.83	1.56	0.16	—	35.89	1.45	—	24.64	—
	[110]	4.66	1.99	1.01	9.34	32.32	9.15	84.09	3.53	0.38
	[111]	42.06	9.74	4.75	6.96	331.22	42.77	62.60	7.74	5.28
VC	[100]	6.84	2.62	1.03	—	46.30	9.28	—	4.98	—
	[110]	14.14	4.61	2.52	4.93	100.06	22.69	44.41	4.40	2.25
	[111]	10.70	5.29	2.66	2.04	65.39	24.01	18.42	2.72	3.55
NbC	[100]	4.22	1.67	0.30	—	27.39	2.74	—	9.97	—
	[110]	4.87	2.26	1.58	7.06	29.51	14.28	63.59	2.06	0.46
	[111]	16.04	5.69	3.60	3.39	108.20	32.47	30.54	3.33	
TaC	[100]	4.27	1.75	0.37	—	28.47	3.33	—	8.53	—
	[110]	5.35	2.43	1.74	6.57	34.38	15.69	59.18	2.19	0.58
	[111]	12.99	5.18	3.36	2.88	87.51	30.31	25.98	2.88	3.36

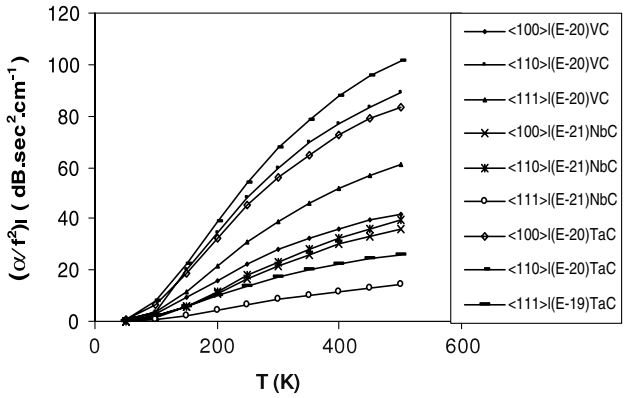

Figure 2. Temperature variation of $(\alpha/f^2)_l$ along different directions of propagation of group V carbides.

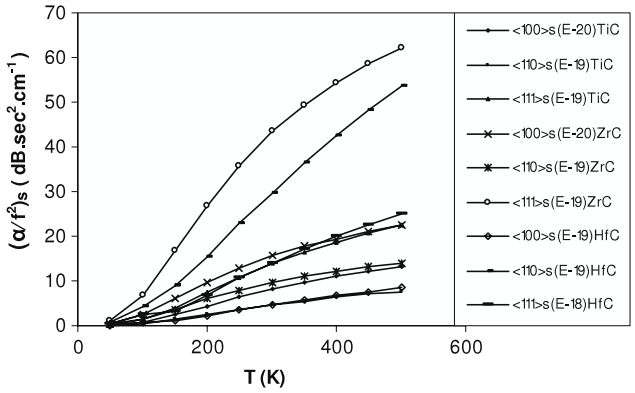

Figure 3. Temperature variation of $(\alpha/f^2)_s$ along different directions of propagation of group V carbides (individual curves have different powers which are depicted on the right-hand side of the figure). Curve along ⟨100⟩ (—◇—) for HfC and along ⟨110⟩ (—•—) for TiC overlap and curves along ⟨111⟩ (—▲—) for TiC and along ⟨100⟩ (—×—) for ZrC overlap.

Temperature variation of ultrasonic attenuation due to thermoelastic loss, $(\alpha/f^2)_{th}$ (obtained using equation (8)), is shown in figures 5 and 6. From figures 1–6, it can be seen that (α/f^2) due to thermoelastic loss is about 2–5% of that due to the phonon–phonon interaction, because the larger part of the acoustical energy is used up in establishing thermal phonon equilibrium. The temperature variation of the phonon relaxation time calculated using equation (4) is shown in figures 7 and 8.

One well-known source of energy loss due to thermal phonons is the thermoelastic loss that occurs because the compressed regions are at higher temperatures compared to rarefied regions. Thus heat transfer from hotter to colder regions gives larger thermoelastic loss in the low temperature region [24]. The rate of change of $(\alpha/f^2)_l$ and $(\alpha/f^2)_s$ with temperature is small in the temperature range 50–200 K (figures 1–4) due to a smaller rate of transfer of energy from acoustical phonons to thermal phonons at a rate E_0 (figure 9). In the temperature range 50–200 K, the energy density, E_0, is small enough to result in less p–p interaction in these TMCs, causing small attenuation due to p–p interaction. Phonon–phonon interaction increases rapidly at a constant rate with temperature like the variation of E_0 with temperature. Therefore attenuation due to p–p interaction increases rapidly, while $(\alpha/f^2)_{th}$ becomes constant due to establishment of an equilibrium condition between compressed and rarefied regions. Therefore, $(\alpha/f^2)_l$ and $(\alpha/f^2)_s$ increase rapidly and $(\alpha/f^2)_{th}$ becomes constant in the high temperature range (200–500 K). Thus, the temperature variation of (α/f^2) in these TMCs are mainly affected by energy density, E_0, and follow similar trend.

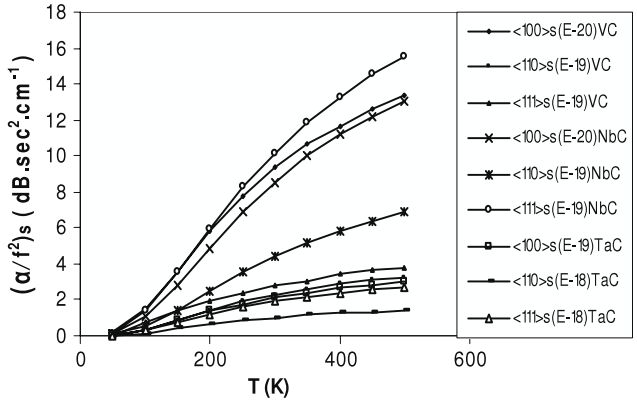

Figure 4. Temperature variation of $(\alpha/f^2)_s$ along different directions of propagation of group V carbides (individual curves have different powers as depicted on the right-hand side of the figure).

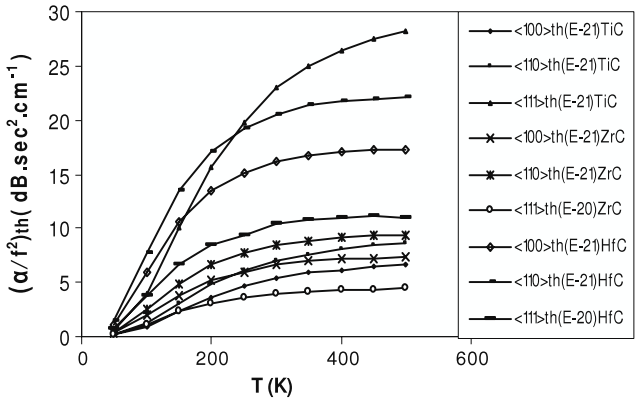

Figure 5. Temperature variation of $(\alpha/f^2)_{th}$ along different directions of propagation of group IV carbides (individual curves have different powers as depicted on the right-hand side of the figure).

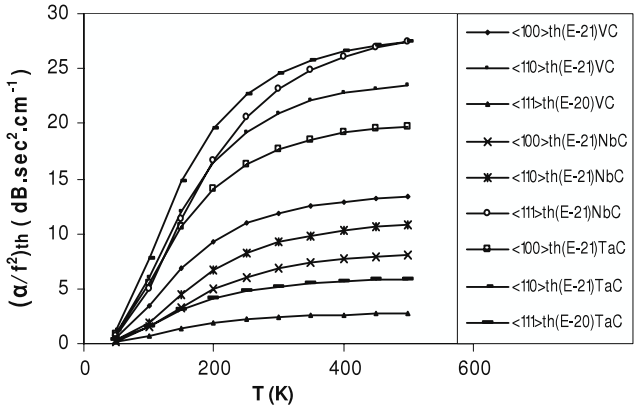

Figure 6. Temperature variation of $(\alpha/f^2)_{th}$ along different directions of propagation of group V carbides (individual curves have different powers as depicted on the right-hand side of the figure).

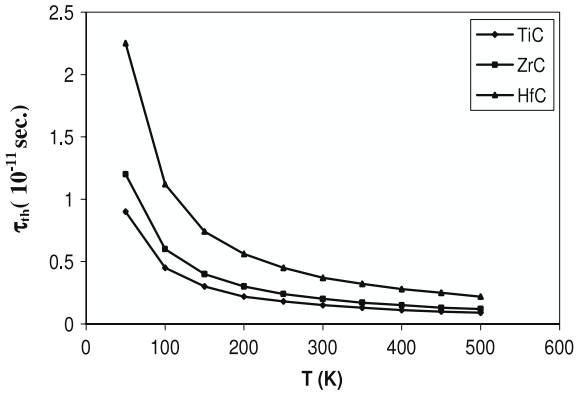

Figure 7. Temperature variation of thermal relaxation time (τ_{th}) of group IV carbides.

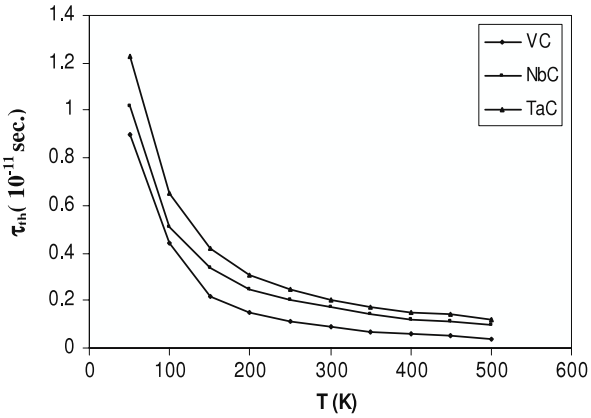

Figure 8. Temperature variation of thermal relaxation time (τ_{th}) of group V carbides.

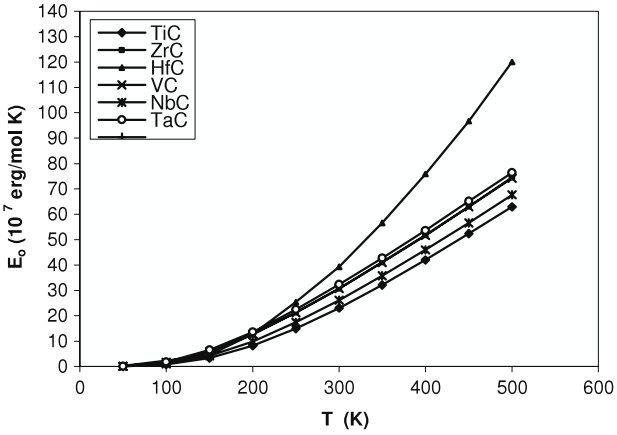

Figure 9. Temperature variation of lattice energy density (E_0) of group V and VI carbides. Curve for ZrC (—■—) and VC (—×—) overlap, i.e. the energy density for these compounds is nearly the same.

(α/f^2) for longitudinal and shear waves due to thermoelastic loss is large along [111] in comparison to along the [100] and [110] directions, due to the fact that the Gruneisen parameters, $\langle \gamma_i^{j2} \rangle$ for longitudinal and shear waves and nonlinearity coupling constants Γ_l, Γ_s and Γ_s^* (which are measures of the anharmonicity of the lattice) have larger values along the [111] and smaller along the [100] and [110] directions (table 3).

4. Conclusions

Elastic moduli obtained at different temperatures using electrostatic and Born repulsive potentials have been used to study the ultrasonic attenuation properties of transition metal carbides. Our calculated values for second-order elastic moduli C_{11}, C_{12} and C_{44} for B1 type TMCs are in good agreement with the available experimental results. Temperature-dependent ultrasonic attenuation, induced by p–p interaction, thermoelastic loss and dislocation damping due to screw and edge dislocations in TMCs shows that the attenuation is mainly governed by phonon–phonon interaction, which is mainly dependent on the variation of energy density, E_0, and attenuation due to thermoelastic loss and dislocation damping is negligible.

Temperature variation of ultrasonic attenuation, $(\alpha/f^2)_l$ and $(\alpha/f^2)_s$, obey the Gaussian fitting law (figures 1–4) and $(\alpha/f^2)_{th}$ follows this variation:

$$(\alpha/f^2)_{th} = (\alpha/f^2)_0 + A\exp(-T/t) \tag{10}$$

where $(\alpha/f^2)_0$ is constant (in units of $(\alpha/f^2)_{th}$, and A and t are also constants). The phonon relaxation time shows the exponential decay with temperature (figures 7 and 8). Although no comparison has been made due to the lack of reported attenuation values in the literature, yet the agreement in values of elastic constants and the nature of ultrasonic attenuation in other similar materials justify the present approach.

Acknowledgment

One of us (RKS) is grateful to the University Grants Commission, New Delhi, Government of India for financial assistance.

References

[1] Isaev E I, Simak S I, Abricosove I A, Ahuja R, Vekilov Yu Kh, Katsnelson M I, Lichtenstein A I and Johansson B 2007 *J. Appl. Phys.* **101** 123519
[2] Sahnoun M, Daul C, Driz M, Parlebas J C and Demangeat C 2005 *Comput. Mater. Sci.* **33** 175–85
[3] Swapnil S and Dahotre Narendra B 2002 *Mater. Manuf. Process* **17** 1–12
[4] Lu X-G, Malin S and Sundman B 2007 *Acta Mater.* **55** 1215–26
[5] Wolf W, Podlouckey R, Antretter T and Fischer F D 1999 *Phil. Mag.* B **79** 839–58
[6] Wu Z, Chen X-J, Struzhki Victor V and Roneld E 2005 *Phys. Rev.* B **71** 214103
[7] Zhao L R, Chen K, Yang Q, Rodgers J R and Chiou S H 2005 *Surf. Coat. Technol.* **200** 1595–9
[8] Yilbas B S, Arif A F M, Karatas C and Ahsan M 2007 *Appl. Surf. Sci.* **253** 5544–52
[9] Akhiezer A 1939 *J. Phys. (USSR)* **1** 227
[10] Kor S K and Singh R K 1993 *Acustica* **79** 83
[11] Kor S K, Kailash K S and Mehrotra P J 1987 *J. Phys. Soc. Japan* **56** 2428
[12] Singh R K and Pandey K K 2006 *Acta Physica Pol.* A **109** 219
[13] Singh R K, Singh R and Singh M P 2007 *ICA-2007: Proc. 19th Int. Congress on Acoustics (Madrid)*
[14] Mason W P 1967 *J. Acoust. Soc. Am.* **42** 253
[15] Mason W P and Rosenberg A 1969 *J. Acoust. Soc. Am.* **45** 470
[16] Mason W P and Bateman T B 1964 *J. Acoust. Soc. Am.* **36** 645
[17] Mason W P 1965 *Physical Acoustics* vol 3 B (New York: Academic)
[18] Nava R and Romro J 1978 *J. Acoust. Soc. Am.* **64** 529
[19] Woodruff T O and Enhereich H 1961 *Phys. Rev.* B **123** 1553
[20] Mason W P 1964 *Physical Acoustics* vol 3B, ed W P Mason and R N Thurston (New York: Academic) chapter 6
[21] Brugger K 1964 *Phys. Rev.* A **133** 1611
[22] Leibried G and Hahn Zur H Z 1958 *Phys. Rev.* B **150** 497
[23] Ludwig W and Leibfried G 1967 *Solid State Physics* vol 12 (New York: Academic)
[24] Sahasrabudhe G G and Lambade S D 1998 *J. Acoust. Soc. Am.* **104** 81